


ENVIRONMENTAL RESEARCH
LETTERS

LETTER

Carbon dioxide release from retrogressive thaw slumps in Siberia

OPEN ACCESS

C Beer^{1,2,*} , A Runge³, G Grosse^{3,4}, G Hugelius^{5,6} and C Knoblauch^{1,2}RECEIVED
7 July 2023REVISED
11 September 2023ACCEPTED FOR PUBLICATION
27 September 2023PUBLISHED
10 October 2023¹ Department of Earth System Sciences, Institute of Soil Science, Universität Hamburg, 20146 Hamburg, Germany² Center for Earth System Research and Sustainability, Universität Hamburg, 20146 Hamburg, Germany³ Permafrost Research Section, Alfred Wegener Institute Helmholtz Centre for Polar and Marine Research, 14473 Potsdam, Germany⁴ Institute of Geosciences, University of Potsdam, 14476 Potsdam, Germany⁵ Department of Physical Geography, Stockholm University, 10691 Stockholm, Sweden⁶ Bolin Centre for Climate Research, Stockholm University, 10691 Stockholm, Sweden

* Author to whom any correspondence should be addressed.

E-mail: christian.beer@uni-hamburg.deOriginal content from
this work may be used
under the terms of the
[Creative Commons
Attribution 4.0 licence](https://creativecommons.org/licenses/by/4.0/).**Keywords:** permafrost, organic matter, respiration, hillslopeSupplementary material for this article is available [online](#)Any further distribution
of this work must
maintain attribution to
the author(s) and the title
of the work, journal
citation and DOI.**Abstract**

Thawing of ice-rich permafrost soils in sloped terrain can lead to activation of retrogressive thaw slumps (RTSs) which make organic matter available for decomposition that has been frozen for centuries to millennia. Recent studies show that the area affected by RTSs increased in the last two decades across the pan-Arctic. Combining a model of soil carbon dynamics with remotely sensed spatial details of thaw slump area and a soil carbon database, we show that RTSs in Siberia turned a previous quasi-neutral ecosystem into a strong source of carbon dioxide of 367 ± 213 gC m⁻¹ a⁻¹. On a global scale, recent CO₂ emissions from Siberian thaw slumps of 0.42 ± 0.22 Tg carbon per year are negligible so far. However, depending on the future evolution of permafrost thaw and hence thaw slump-affected area, such hillslope processes can transition permafrost landscapes to become a major source of additional CO₂ release into the atmosphere.

1. Introduction

Air temperature in the Arctic is rising almost four times faster than the global mean due to the Arctic amplification of global warming (Rantanen *et al* 2022). This accelerated warming is a strong driver of thawing terrestrial permafrost (Biskaborn *et al* 2019, Smith *et al* 2022), especially of a gradual deepening of the active layer (Park *et al* 2016, Peng *et al* 2016). Furthermore, disturbances to soil layers which insulate the permafrost, including fires or other damage to organic soils horizons or vegetation, as well as changing snow dynamics (Porada *et al* 2016, Beer *et al* 2018, Heim *et al* 2022) can cause even more rapid thaw through additional alteration of the soil thermal regime. Especially in locations with a high amount of segregated and unevenly distributed ground ice, such as large ice wedges, or massive remnants of buried glacial ice, melting can result in a drastic change of the ground leading to rather rapid and abrupt permafrost landscape changes (Nitzbon *et al* 2020) such as thermo-erosional gullies and valleys (Morgenstern

et al 2021), thermokarst lake dynamics (Grosse *et al* 2013), coastal erosion (Günther *et al* 2013), or retrogressive thaw slumps (RTSs) (Burn and Lewkowicz 1990). Both processes, gradual and abrupt thawing, lead to widespread landscape changes in permafrost regions and pose a threat to Arctic communities and infrastructure, ecosystems, and carbon pools, but differ in spatial and temporal scales.

Currently, only gradual permafrost thaw is accounted for in global climate models. While gradual thaw impacts a larger region than abrupt thaw, Turetsky *et al* (2019) estimated that greenhouse gas emissions from abrupt thaw will increase permafrost carbon release projections, which are based on gradual thaw, for 2300 by about 50%, hence contributing substantially to greenhouse gas emissions from permafrost regions. The pan-Arctic area of such ground failures and landscape changes due to permafrost thawing and the resulting alteration of the carbon cycle processes are still unclear. Combining broad-scale remote sensing approaches to determine landscape scale changes from permafrost thaw with

modelling of carbon dynamics will help quantifying the impacts of abrupt thaw at continental scales. For example, Runge *et al* (2022) estimated the area of RTS in Siberia during the past two decades (1999–2020) based on high resolution remote sensing data across an 8 million km² study region. Such datasets provide a unique opportunity to explore the scaling of field measured greenhouse fluxes from RTS with numerical modelling.

RTS result from slope failure due to abrupt thawing of ice-rich permafrost. They mostly occur along shorelines of lakes, rivers, and coastlines. They are mass-wasting features, which after initial detachment failure and the exposure of ice-rich soils consist of a headwall, a muddy slump floor and often a drainage channel. The slope-failure processes associated with RTS formation and growth expose permafrost soil layers that have been frozen in the deep subsoil for hundreds or thousands of years. In RTS, these layers become part of the active layer and erode quickly due to the thermo-erosional processes driving RTS growth. Mudflows, originating from the headwalls, flow across the thaw slump floors and usually exit through small meltwater gullies into downstream environments such as lakes, streams, or the Arctic Ocean (Lantuit and Pollard 2005). As a consequence, previously frozen terrestrial organic matter will be partly exported to aquatic systems and further processed in there (Beel *et al* 2020, Kokelj *et al* 2021). In addition, microbes will start to mineralize the organic matter that has been frozen for a long time and is exposed in RTS, releasing greenhouse gases such as carbon dioxide or methane (Knoblauch *et al* 2021). The geomorphological and biogeochemical processes in RTS have the potential to release greenhouse gases from thawing permafrost much faster than due to a gradual deepening of the active layer. For instance (Knoblauch *et al* 2021) estimated a CO₂ release of 160–180 gC m⁻¹ a⁻¹ from a RTS in Northeast Siberia. In this study, we focus on the CO₂ release from the RTS soils, i.e. material that has not been exported to aquatic systems.

At a continental to global scale, detailed estimates of CO₂ release from RTS based on combined field studies, remote sensing and models are lacking. In this study, we integrate a dynamic decomposition model with a recent remote sensing map and a soil carbon database to estimate recent carbon dioxide emissions from RTS in Siberia. The following research questions are addressed:

(1) What is the amount of previously frozen soil organic matter available for mineralization due to recent RTS development at the continental-scale in Siberia? (2) How much CO₂ has potentially been recently released from to RTSs to the atmosphere in Siberia in 1999–2020? (3) Has this estimated additional carbon release to the atmosphere any impact on the global carbon cycle?

2. Methods

2.1. Estimation of organic matter mineralization at thaw slumps

We estimated the amount of annually mineralized organic matter which is released as CO₂ to the atmosphere using a dynamic 2-pool first-order decomposition model implemented in MathWorks MATLAB R2022b following Andr en and K atterer (1997) and Beer *et al* (2022). Model parameters were taken from Knoblauch *et al* (2013). To account for soil temperature seasonality and vertical distribution, we assumed the decomposition rate constant k being temperature dependent following a Q₁₀-model (equation (1)):

$$k = k_{\text{ref}} \cdot Q^{\frac{T - T_{\text{ref}}}{10}} \quad (1)$$

where k_{ref} are the parameter values taken from Knoblauch *et al* (2013), and T_{ref} is the corresponding temperature (4 °C). We assumed the parameter Q equals to 2 (Sch adel *et al* 2016, Vaughn and Torn 2019).

We applied this model to all detected RTS across the entire study area in Siberia. The model required several variables as input (see sections below): location and area of the thaw slumps, mean soil temperature seasonality for topsoil and subsoil, and initial soil organic carbon stocks. Based on the availability of soil temperature data, we conducted the calculations at a 0.5° grid cell scale. First we defined a 0.5° grid and determined for each cell the areal fraction of RTS, topsoil and subsoil temperature monthly means, and initial soil organic matter content. Then, the dynamic model has been run using these boundary conditions.

We accounted for uncertainty of model parameters using all the 48 parameter sets from Knoblauch *et al* (2013) representing Holocene and Pleistocene soils from Kurungnakh (supplemental material). The uncertainty of thaw slump area correction and soil organic matter stocks were reported as standard deviations. For each grid cell we resampled a normal distribution representing that standard deviation and the means of area and organic matter stocks using a vector of ten values for both variables. As a result, we estimated carbon emissions 4800 times for each 0.5 grid cell and reported the mean and standard deviation of all these results from all grid cells.

2.2. RTS area estimation

Active RTS were mapped across Northeast Siberia firstly to identify their distribution at continental scale, secondly to derive their annual thaw dynamics from 1999 to 2020, and thirdly to determine the terrestrial area currently impacted by rapid thaw from thaw slumps. To achieve this, we applied the Landsat-based detection of Trends in Disturbance and Recovery (LandTrendr) algorithm, which performs spectral-temporal segmentation from time

series data to identify disturbance events and recovery periods from annual Landsat mosaics (Kennedy *et al* 2010). The algorithm is implemented as LandTrendr-Google Earth Engine (Kennedy *et al* 2018). We adapted and parameterised the LT-GEE algorithm to be sensitive to the spectral change associated to RTS thawing dynamics and to detect their annual thawing dynamics in Northeast Siberia (Runge *et al* 2022).

Firstly, we expanded the data scope from Landsat-only to also include Sentinel-2 images for an improved study area coverage in the northern high latitudes (Runge and Grosse 2020), and implemented spectral band adjustments between Sentinel-2 and Landsat for harmonized Landsat and Sentinel-2 annual mosaics (Runge and Grosse 2019). Secondly, we created ground truth data of individual RTS in the study area with TimeSync (Cohen *et al* 2010) to parameterise the required run parameters of LT-GEE based on the tasselled cap greenness spectral index (Huang *et al* 2002). Lastly, we ran LT-GEE with this parameterisation for the study area for the time period 1999–2020. Additionally, we performed spatial masking and a binary classification to limit the LT-GEE results to RTS and exclude other disturbances with a similar spectral signature, such as fire scars and landslides. With this, the adapted LT-GEE identifies the change in spectral signature associated to the change of land cover from (intact) vegetation to bare soil and ground due to thaw slumping within the assessment period. Therefore, the results represent active RTS as in newly disturbed area resulting from initiation, re-initiation of stabilised RTS, and lateral growth of RTS from 2000 to 2019. This mapping approach cannot detect and consider old, stabilised and revegetated RTS as their spectral signature differs strongly. It further neglects stabilisation and vegetation encroachment and succession within the RTS potentially following a disturbance within the assessment period. In total, 50 895 active RTS were identified, which affected a total area of 868 57 km² by 2020. The mapped active RTS vary in size with a mean size of 1.7 ha. The smallest and largest mapped RTS were constrained by a minimum (0.36 ha) and maximum (15 ha) mapping unit, which had to be applied to ensure reliable RTS mapping. These RTS sizes overall agree well with other studies stating RTS sizes ranging from 0.15 ha to 52 ha of mega slumps (Günther *et al* 2015, Kokelj *et al* 2015, Lacelle *et al* 2015, Ramage *et al* 2017). There is a small bias towards larger slumps following Landsat's 30 m spatial resolution but the most commonly occurring RTS sizes are captured. The temporal analysis of rapid thaw dynamics showed initially an overall steady increase in RTS-affected area in Northeast Siberia with a more abrupt increase from 2016 onward (Runge *et al* 2022).

The RTS area derived from Landsat and Sentinel-2 data (30 m resolution) was then validated with very high resolution (VHR) multispectral RapidEye (RE)

imagery (5 m resolution) across the study area for 2018 and 2019. The resulting bias and uncertainty range of the 30 m resolution product were used to correct the initial thaw slump area estimate. VHR multispectral imagery is limited due to frequent cloud cover and the large extent of the study area, hence we performed the validation on five focus sites across the study area.

2.3. Soil organic carbon stocks at 0.5° grid cell scale

The data on spatial distribution of soil organic carbon stocks is derived from the Northern Circumpolar Soil Carbon Database, version 2 (NCSCDv2; see Hugelius (Hugelius *et al* 2013, 2014)). This dataset was created by combining several different national or regional soil classification maps across the northern permafrost region with field-based soil profile data. The coverage of different soil types from polygon-based soil classification maps were digitized into a Geographic Information System and harmonized to a common soil classification scheme, the United States Department of Agriculture Soil Taxonomy (Soil Survey Staff 1999). At the regional scale, the soil map coverage was then linked to soil profile data (total profile $n = 1778$) to calculate soil organic carbon storage for different standard depth intervals. The data was then gridded to several different grid cell resolutions. For the analyses in this study, data for 0–100 cm depth at a grid-cell resolution of 0.5° was used. The 30% and 70% of total 0–100 cm organic matter stocks were assigned to topsoil and subsoil stocks, respectively.

2.4. Soil temperature profile at 0.5° grid cell scale

The time series of the temperature profile at 0.5° grid cells that show RTS during 1991–2010 has been estimated by a pan-Arctic simulation using the land surface model JSBACH. This model has recently been advanced by including cold regions processes (Ekici *et al* 2014, Beer *et al* 2018, 2020). For this study, we run a model version that does not consider a layer of lichens and bryophytes because such layer is missing at the disturbed RTS sites. In total, five dynamic snow layers, and seven soil layers were used in an implicit numerical scheme to solve the heat conduction equation with phase change. Depth of thermal and hydrological layers increase from 6 cm at the surface to 30 m for the bottom layer reaching a total depth of 53 m. The horizontal resolution of the model results is 0.5° following the resolution of climate forcing data. JSBACH interpolates daily climate forcing data to half-hourly values which is the internal time step of the model. The 0.5° climate data set for the period 1901–2100 is a combination of observation-based and reanalysis data sets as well as Earth System Model results. Details about the data set and the bias-correction method are given in Beer *et al* (2020). This model version has been intensively evaluated in terms

of cold regions physical processes at site level and pan-Arctic scale (Ekici *et al* 2014, Porada *et al* 2016, Beer *et al* 2018, 2020), and in particular also for a specific RTS in Northeast Siberia (Knoblauch *et al* 2021). For the estimation of heterotrophic organic matter mineralization we averaged temperature at soil layers for topsoil 0–30 cm and subsoil 30–100 cm for each grid cell. While soil temperature can be highly variable among and within RTS due to slope orientation and aspect (Turner *et al* 2021), we here use a landscape-scale mean at 0.5° grid cell size in order to cover the seasonality and large-scale variation in soil temperature.

3. Results

3.1. RTS area correction

The comparison of the identified RTS to VHR images showed an average underestimation of the area impacted by rapid thaw by 2020 of 32.5% with a standard deviation of 26%. This area underestimation by LT-GEE can be explained by three aspects: Firstly, the spatial resolution of the combined Landsat and Sentinel-2 data sets (30 m) differs to the VHR RE images by one order of magnitude, leading to area gaps, especially at the boundaries of individual RTS due to the 30 m pixel size. Secondly, overall we underestimate the area affected by RTS in Northeast Siberia as we are restricted to a minimal mapping unit of 0.36 ha. RTS are overall small-scale disturbance features with typical slump sizes ranging from 0.15 ha to a few hectares (Kokelj *et al* 2015, Lacelle *et al* 2015). Because of this, our mapping approach with LT-GEE misses the smaller scale disturbances. Thirdly, (Runge *et al* 2022) only assessed active RTS dynamics between 1999–2020 and thaw dynamics before this assessment period could not be accounted for with LT-GEE. However, when delineating RTS boundaries, the RTS area in VHR RE images contains the full disturbance scar, and also sediment flow tracks were mostly included as they are considered a part of a RTS. As these areas were disturbed before 1999 or as in the case for the sediment flow tracks remain constantly disturbed from a spectral point of view (no change from intact vegetation to bare soil) these areas are not picked up as disturbances with LT-GEE from 1999 to 2020 (which may pre-date 1999). We therefore correct each individual RTS area by this bias of $32 \pm 26\%$ resulting in a total area of $1145 \pm 2.5 \text{ km}^2$.

3.2. Soil organic carbon availability at RTS

Based on the NCSCDv2 we estimated the amount of soil organic carbon of the upper meter of soil of all RTS individually. Due to the exponential distribution of the thaw slump area (Runge *et al* 2022), also the total amount of soil organic carbon follows this distribution (figure 1(a)). The absolute amount of organic carbon lies in between $0.05 \times 10^6 \text{ kg C}$ and

$43 \times 10^6 \text{ kg C}$ with a mean of $1.25 \times 10^6 \text{ kg C}$ in the first meter of soil. Based on this approach, a total of 29 Tg C are currently present within the first meter of soil in all these mapped thaw slumps in Siberia. The mean carbon content per m^2 of ground is shown in figure 1(b). This is the direct extract for the individual thaw slumps from the NCSCDv2. It is important to note the high organic carbon content in the West Siberian lowlands (peatlands), in the Yedoma regions of Yakutia and the Far East (Strauss *et al* 2017) and along rivers due to repeated alluvial deposition. In the southern mountain regions, organic carbon content is lower, which must be taken into account when interpreting the results of CO_2 emissions.

3.3. Topsoil and subsoil temperature at RTS

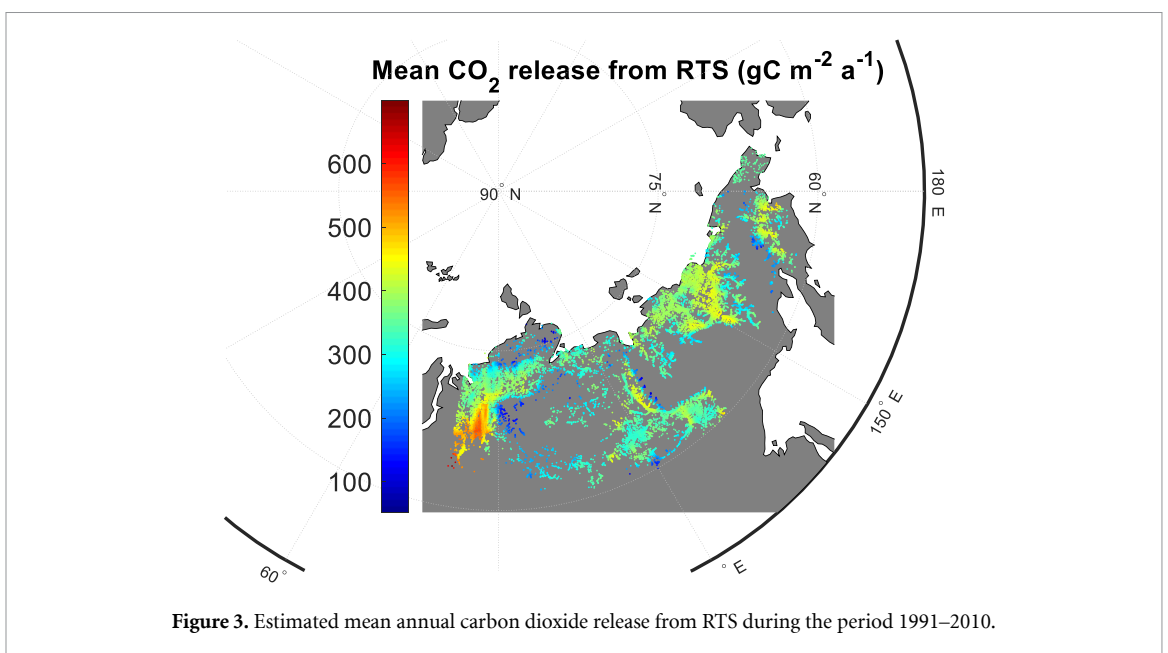
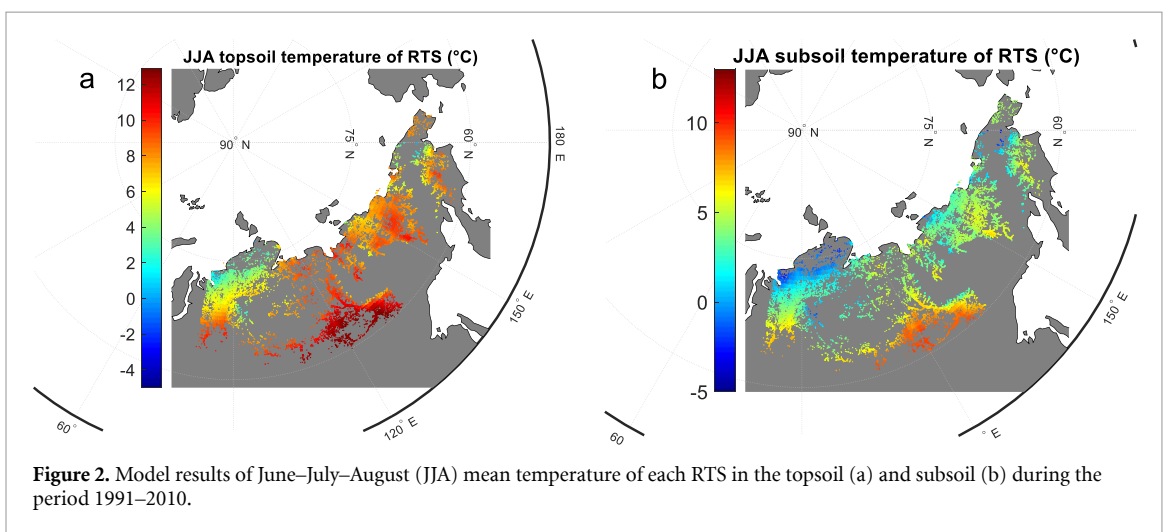
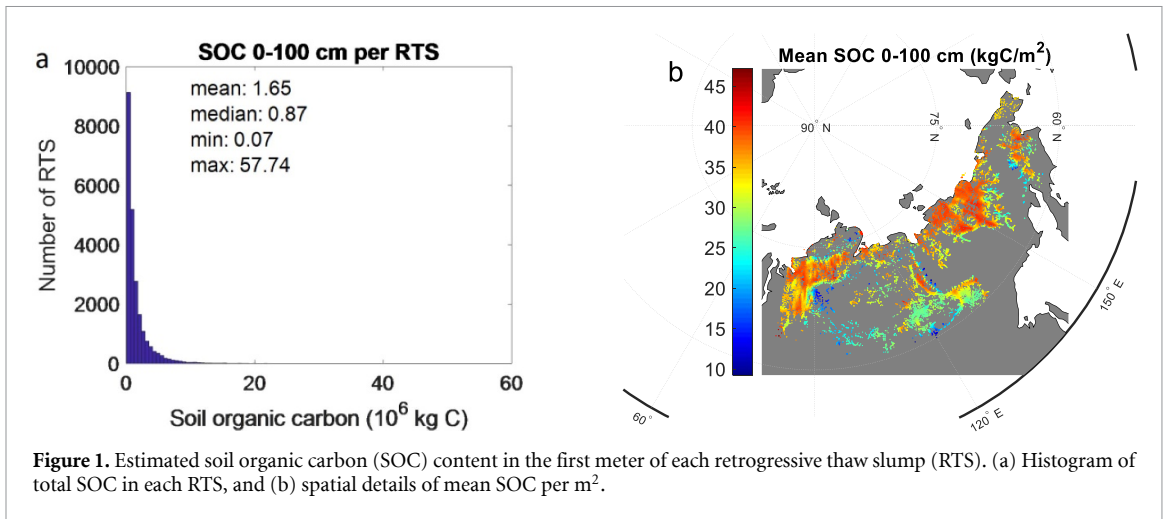
The offline simulations by the land surface model JSBACH result in current topsoil temperatures of 0°C – 12°C in summer (June–July–August) with clear latitudinal and longitudinal gradients (figure 2(a)). Soil temperature higher than 10°C in southern West Siberia and in Yakutia are responsible for a substantial CO_2 production. Subsoil temperature (30–100 cm) can be also below the freezing point in northern regions depending on the active layer thickness (figure 2(b)). This may limit organic matter decomposition. However, many RTS show a positive subsoil temperature as a mean for 30–100 cm in summer (figure 2(b)).

3.4. Carbon dioxide release from RTS

When applying the dynamic decomposition model to the available soil organic matter with the specific topsoil and subsoil temperature, we estimate a mineralization of organic matter of $367 \pm 213 \text{ g C m}^{-1} \text{ a}^{-1}$ on average for all RTS (figure 3). This corresponds to a total CO_2 release to the atmosphere of $0.42 \pm 0.22 \text{ TgC/a}$ from all these thaw slumps in Siberia.

4. Discussion

Thawing ice-rich permafrost can lead to abrupt thermokarst and fluvio-thermal erosion and substantial change of the landscape geomorphology. In hillslope regions, these processes can result in the formation of RTSs. Such thaw slumps make previously permanently frozen organic matter, often many millennia old, available for microbial decomposition by rapidly transporting these subsoil layers towards the exposed and warm surface. Is this locally abundant and often dramatic phenomenon important at the continental scale for the global carbon cycle? To address this question, we for the first time combined several novel datasets about RTS (remotely sensed area, soil carbon database, CO_2 production studies) with dynamic modelling to estimate the recent Siberian carbon emission from these thaw slumps.



Our results show that these RTS are a strong carbon source (local hotspot) to the atmosphere. The average emission of $367 \pm 204 \text{ gC m}^{-1} \text{ a}^{-1}$ is in stark

contrast to an otherwise small carbon sink of the tundra in this area (Eckhardt *et al* 2019). However, the recent RTS-affected area in Siberia of 868 km^2

is not large enough for emissions to be relevant for the global carbon cycle. The estimated carbon emission of 0.42 TgC/a from these Siberian thaw slumps is four orders of magnitude lower than the annual anthropogenic carbon emissions of about 10.6 PgC/a (Friedlingstein *et al* 2022). Nevertheless, the large amount of CO₂ emitted from a relatively small, but rapidly increasing RTS area, is concerning for future scenarios should this RTS growing trend since 2016 continue. RTS area growth for North Siberia from 1999 to 2019 has exceeded 331% (Runge *et al* 2022). This substantial growth rate for Siberian RTS area is met with similar high rates observed over recent decades in smaller regions of NW Canada, such as the Mackenzie Delta region (+2% to +407% from 1950/1960s to 2004/2008) (Segal *et al* 2016) or Banks Island (increase in RTS numbers by 6370% from 1984 to 2015) (Lewkowicz and Way 2019).

If we assumed a constant RTS area and constant related available organic matter in the future, then our results suggest a CO₂ emission of 0.54 TgC/a at the end of the century due to soil warming following the RCP8.5 scenario (481 gC m⁻¹ a⁻¹, data not shown). This means that also future soil warming will have a minor effect on CO₂ emissions from RTS. However, the RTS-affected area may change dramatically with ongoing warming especially in the high Arctic as many recent studies suggest a close relation of rapid permafrost thaw to extreme climate events such as extreme summer temperatures or precipitation (Lantz and Kokelj 2008, Kokelj *et al* 2015, Farquharson *et al* 2019, Lewkowicz and Way 2019, Ward Jones *et al* 2019, Bernhard *et al* 2022). A further important aspect is that RTS volumes are difficult to estimate from optical remote sensing data and require digital elevation data that allows more detailed estimates of mobilized sediment volumes and carbon (Bernhard *et al* 2022). Based on the RCP8.5 scenario, Turetsky *et al* (2020) assume an increase of pan-Arctic active thaw slump area from 1797 km² in the year 2000 via 15 725 km² in 2025 to 62 933 km² in 2100 (RCP8.5). If we assumed this area of 62 933 km² in 2100, then we would predict a CO₂ emission from RTS to the atmosphere of 30.2 TgC/a at the end of the century. Using a linear model of an increase from 0.4 to 30.2 TgC/a during 80 years integrates to an overall total amount of 1.2 Pg carbon that could be emitted to the atmosphere just from these RTSs alone. This number is lower than the 4.4 PgC estimated by Turetsky *et al* (2020), but confirms the previously published order of magnitude, and that RTS can have an important contribution to the future carbon release from thawing permafrost. These back-at-the-envelope calculations demonstrate that the main source of uncertainty of such prediction of future greenhouse gas releases from RTS is due to the high uncertainty of future thaw slump area. Therefore, further research on dynamic modelling

of segregated ice content in permafrost-affected soils and related thermo-erosion processes is required.

5. Conclusions

RTSs in Siberia represent a major hotspot of carbon dioxide release into the atmosphere. Essentially, such lateral thermo-erosion and subsidence following ice-rich permafrost thaw alters the carbon balance of permafrost-affected ecosystems from a small sink to a strong source of CO₂. On a global scale, the resulting recent carbon release is negligible compared to other global carbon cycle processes so far. In the future, however, it may become more substantial, depending on the dynamics of affected areas having ice-rich permafrost.

Data availability statement

The data that support the findings of this study are openly available at the following URL/DOI: <https://zenodo.org/record/7552550> (doi: <https://doi.org/10.5281/zenodo.7552550>).

Acknowledgments

C B acknowledges financial support by DFG-BE 6485/1-1 and DFG-BE 6485/4-1. C K was supported by the German Ministry of Education and Research (KOPF-Synthesis Project 03F0834A) and the DFG excellence cluster CLICCS (EXC2037/1). We acknowledge the technical support by CEN-IT which is the central IT service provider of the Center for Earth System Research and Sustainability at Universität Hamburg. A R was supported by an ESA CCI Postdoctoral Fellowship. G G and A R acknowledge support by ESA CCI+ Permafrost, EU Horizon 2020 project Arctic Passion (Grant No. 101003472), and the BMBF KoPf Synthesis project (03F0834B).

Conflict of interest

All authors declare no conflict of interest.

ORCID iD

C Beer  <https://orcid.org/0000-0002-5377-3344>

References

- Andr n O and K tterer T 1997 ICBM: the introductory carbon balance model for exploration of soil carbon balances *Ecol. Appl.* **7** 1226–36
- Beel C R, Lamoureux S F, Orwin J F, Pope M A, Lafreni re M J and Scott N A 2020 Differential impact of thermal and physical permafrost disturbances on high Arctic dissolved and particulate fluvial fluxes *Sci. Rep.* **10** 11836
- Beer C, Knoblauch C, Hoyt A M, Hugelius G, Palmtag J, Mueller C W and Trumbore S 2022 Vertical pattern of organic matter decomposability in cryoturbated permafrost-affected soils *Environ. Res. Lett.* **17** 104023

- Beer C, Porada P, Ekici A and Brakebusch M 2018 Effects of short-term variability of meteorological variables on soil temperature in permafrost regions *Cryosphere* **12** 741–57
- Beer C, Zimov N, Olofsson J, Porada P and Zimov S 2020 Protection of permafrost soils from thawing by increasing herbivore density *Sci. Rep.* **10** 4170
- Bernhard P, Zwieback S and Hajnsek I 2022 Accelerated mobilization of organic carbon from retrogressive thaw slumps on the northern Taymyr Peninsula *Cryosphere* **16** 2819–35
- Biskaborn B K et al 2019 Permafrost is warming at a global scale *Nat. Commun.* **10** 264
- Burn C R and Lewkowicz A G 1990 Canadian landform examples—17 retrogressive thaw slumps *Can. Geogr.* **34** 273–6
- Cohen W B, Yang Z G and Kennedy R 2010 Detecting trends in forest disturbance and recovery using yearly Landsat time series: 2. TimeSync—tools for calibration and validation *Remote Sens. Environ.* **114** 2911–24
- Eckhardt T, Knoblauch C, Kutzbach L, Holl D, Simpson G, Abakumov E and Pfeiffer E-M 2019 Partitioning net ecosystem exchange of CO₂ on the pedon scale in the Lena River Delta, Siberia *Biogeosciences* **16** 1543–62
- Ekici A, Beer C, Hagemann S, Boike J, Langer M and Hauck C 2014 Simulating high-latitude permafrost regions by the JSBACH terrestrial ecosystem model *Geosci. Model. Dev.* **7** 631–47
- Farquharson L M, Romanovsky V E, Cable W L, Walker D A, Kokelj S V and Nicolsky D 2019 Climate change drives widespread and rapid thermokarst development in very cold permafrost in the Canadian high Arctic *Geophys. Res. Lett.* **46** 6681–9
- Friedlingstein P, O'Sullivan M, Jones M W, Andrew R M, Gregor L, Hauck J and Zheng B 2022 Global carbon budget 2022 *Earth Syst. Sci. Data* **14** 4811–900
- Grosse G, Robinson J E, Bryant R, Taylor M D, Harper W, DeMasi A and Harden J W 2013 Distribution of late Pleistocene ice-rich syngenetic permafrost of the Yedoma Suite in east and central Siberia, Russia Open File Report 2013-1078 (U.S. Geological Survey) p 37
- Günther F, Grosse G, Wetterich S, Jones B M, Kunitsky V V, Kienast F and Schirrmeyer L 2015 The batagay mega thaw slump, Yana Uplands, Yakutia, Russia: permafrost thaw dynamics on decadal time scale *Paper presented at the Past Gateways Palaeo-Arctic Spatial and Temporal Gateways*
- Günther F, Overduin P P, Sandakov A V, Grosse G and Grigoriev M N 2013 Short- and long-term thermo-erosion of ice-rich permafrost coasts in the Laptev Sea region *Biogeosciences* **10** 4297–318
- Heim B, Lisovski S, Wiczorek M, Morgenstern A, Juhls B, Shevtsova I, Herzsich U, Boike J, Fedorova I and Herzsich U 2022 Spring snow cover duration and tundra greenness in the Lena Delta, Siberia: two decades of MODIS satellite time series (2001–2021) *Environ. Res. Lett.* **17** 085005
- Huang C, Wylie B, Yang L, Homer C and Zylstra G 2002 Derivation of a tasselled cap transformation based on Landsat 7 at-satellite reflectance *Int. J. Remote Sens.* **23** 1741–8
- Hugelius G et al 2014 Estimated stocks of circumpolar permafrost carbon with quantified uncertainty ranges and identified data gaps *Biogeosciences* **11** 6573–93
- Hugelius G, Tarnocai C, Broll G, Canadell J G, Kuhry P and Swanson D K 2013 The Northern Circumpolar Soil Carbon Database: spatially distributed datasets of soil coverage and soil carbon storage in the northern permafrost regions *Earth Syst. Sci. Data* **5** 3–13
- Kennedy R E, Yang Z G and Cohen W B 2010 Detecting trends in forest disturbance and recovery using yearly Landsat time series: 1. LandTrendr—temporal segmentation algorithms *Remote Sens. Environ.* **114** 2897–910
- Kennedy R E, Yang Z Q, Gorelick N, Braaten J, Cavalcante L, Cohen W B and Healey S 2018 Implementation of the LandTrendr algorithm on Google Earth Engine *Remote Sens.* **10** 691
- Knoblauch C, Beer C, Schuett A, Sauerland L, Liebner S, Steinhof A, Pfeiffer E-M, Grigoriev M N, Faguet A and Pfeiffer E-M 2021 Carbon dioxide and methane release following abrupt thaw of Pleistocene permafrost deposits in Arctic Siberia *J. Geophys. Res.* **126** e2021JG006543
- Knoblauch C, Beer C, Sosnin A, Wagner D and Pfeiffer E-M 2013 Predicting long-term carbon mineralization and trace gas production from thawing permafrost of Northeast Siberia *Glob. Change Biol.* **19** 1160–72
- Kokelj S V, Kokoszka J, van der Sluijs J, Rudy A C A, Tunnicliffe J, Shakil S, Zolkos S and Zolkos S 2021 Thaw-driven mass wasting couples slopes with downstream systems, and effects propagate through Arctic drainage networks *Cryosphere* **15** 3059–81
- Kokelj S V, Tunnicliffe J, Lacelle D, Lantz T C, Chin K S and Fraser R 2015 Increased precipitation drives mega slump development and destabilization of ice-rich permafrost terrain, northwestern Canada *Glob. Planet. Change* **129** 56–68
- Lacelle D, Brooker A, Fraser R H and Kokelj S V 2015 Distribution and growth of thaw slumps in the Richardson Mountains–Peel Plateau region, northwestern Canada *Geomorphology* **235** 40–51
- Lantuit H and Pollard W H 2005 Temporal stereophotogrammetric analysis of retrogressive thaw slumps on Herschel Island, Yukon Territory *Nat. Hazards Earth Syst. Sci.* **5** 413–23
- Lantz T C and Kokelj S V 2008 Increasing rates of retrogressive thaw slump activity in the Mackenzie Delta region, NWT, Canada *Geophys. Res. Lett.* **35** L06502
- Lewkowicz A G and Way R G 2019 Extremes of summer climate trigger thousands of thermokarst landslides in a high Arctic environment *Nat. Commun.* **10** 1329
- Morgenstern A, Overduin P P, Gunther F, Stettner S, Ramage J, Schirrmeyer L, Grosse G and Grosse G 2021 Thermo-erosional valleys in Siberian ice-rich permafrost *Permafr. Periglac. Process.* **32** 59–75
- Nitzbon J, Westermann S, Langer M, Martin L C P, Strauss J, Laboor S and Boike J 2020 Fast response of cold ice-rich permafrost in northeast Siberia to a warming climate *Nat. Commun.* **11** 2201
- Park H, Kim Y and Kimball J S 2016 Widespread permafrost vulnerability and soil active layer increases over the high northern latitudes inferred from satellite remote sensing and process model assessments *Remote Sens. Environ.* **175** 349–58
- Peng S et al 2016 Simulated high-latitude soil thermal dynamics during the past 4 decades *Cryosphere* **10** 179–92
- Porada P, Ekici A and Beer C 2016 Effects of bryophyte and lichen cover on permafrost soil temperature at large scale *The Cryosphere* **10** 2291–315
- Ramage J L, Irrgang A M, Herzsich U, Morgenstern A, Couture N and Lantuit H 2017 Terrain controls on the occurrence of coastal retrogressive thaw slumps along the Yukon Coast, Canada *J. Geophys. Res.* **122** 1619–34
- Rantanen M, Karpechko A Y, Lipponen A, Nordling K, Hyvärinen O, Ruosteenoja K, Laaksonen A and Laaksonen A 2022 The Arctic has warmed nearly four times faster than the globe since 1979 *Commun. Earth Environ.* **3** 168
- Runge A and Grosse G 2019 Comparing spectral characteristics of Landsat-8 and Sentinel-2 same-day data for Arctic-Boreal regions *Remote Sens.* **11** 1730
- Runge A and Grosse G 2020 Mosaicking Landsat and Sentinel-2 data to enhance Landtrendr time series analysis in Northern high latitude permafrost regions *Remote Sens.* **12** 2471
- Runge A, Nitze I and Grosse G 2022 Remote sensing annual dynamics of rapid permafrost thaw disturbances with LandTrendr *Remote Sens. Environ.* **268** 112752
- Schädel C et al 2016 Potential carbon emissions dominated by carbon dioxide from thawed permafrost soils *Nat. Clim. Change* **6** 950–3

- Segal R A, Lantz T C and Kokelj S V 2016 Acceleration of thaw slump activity in glaciated landscapes of the Western Canadian Arctic *Environ. Res. Lett.* **11** 034025
- Smith S L, O'Neill H B, Isaksen K, Noetzi J and Romanovsky V E 2022 The changing thermal state of permafrost *Nat. Rev. Earth Environ.* **3** 10–23
- Soil Survey Staff 1999 *Soil Taxonomy: A Basic System of Soil Classification for Making and Interpreting Soil Surveys* vol Handbook 436, 2nd edn (Natural Resources Conservation Service, U.S. Department of Agriculture)
- Strauss J *et al* 2017 Deep Yedoma permafrost: a synthesis of depositional characteristics and carbon vulnerability *Earth-Sci. Rev.* **172** 75–86
- Turetsky M R *et al* 2020 Carbon release through abrupt permafrost thaw *Nat. Geosci.* **13** 138–43
- Turetsky M *et al* 2019 Permafrost collapse is accelerating carbon release *Nature* **569** 32–34
- Turner K W, Pearce M D and Hughes D D 2021 Detailed characterization and monitoring of a retrogressive thaw slump from remotely piloted aircraft systems and identifying associated influence on carbon and nitrogen export *Remote Sens.* **13** 171
- Vaughn L J S and Torn M S 2019 ¹⁴C evidence that millennial and fast-cycling soil carbon are equally sensitive to warming *Nat. Clim. Change* **9** 467–71
- Ward Jones M K, Pollard W H and Jones B M 2019 Rapid initialization of retrogressive thaw slumps in the Canadian high Arctic and their response to climate and terrain factors *Environ. Res. Lett.* **14** 055006